

ELECTRODYNAMIC FORCES BETWEEN TWO DC BUSBARS DISTRIBUTION SYSTEMS CONDUCTORS

Maria-Catalina PETRESCU¹, Lucian PETRESCU²

This paper analyzes a DC busbar system used in a power distribution unit. The spectrum of the magnetic flux density is investigated for different situations (different distance between the bars) using a comparison between analytical approach and a numerical technique. Also, the forces between the bars are investigated for both normal (rated) and a short-circuit situation. Investigations are performed using analytical and numerical procedures.

Keywords: Busbar, static magnetic field, FEM 2D, electrodynamic forces

1. Introduction

Distribution systems often contained busbar conductors powered in high DC currents [1-2]. These conductors are designed to offer protection to any user, but in an out of ordinary situation this might cause damages to the installations. In this kind of equipments, different problems could appear: magnetic field of medium intensity, high thermal variation, and electrodynamic forces [3].

DC busbar systems are used extensively in the refining of chlorine, resulting products like caustic soda, liquid chlorine, or chlorine dioxide [3]. Another domain of intense usage of these distribution systems is when a high power DC driving utility, like in paper manufacture industry or transportation, is needed.

The aim of this paper is to present an analytical procedure validated by a numerical technique to evaluate the magnetic flux density for a DC busbar distribution system. The electrodynamic forces between those conductors in a rated and high current regime are also evaluated [4]. The main concern appears although when a fault current (like short-circuit) is occurring. In one of these cases, the conductors may suffer mechanical stresses which could generate considerable damages of the entire distribution system [5-8].

The analyzed DC busbar system is presented in Fig. 1. We had considered two rectangular copper conductors with cross section $2a \times 2b$ with the assumption

¹ Faculty of Electrical Engineering, University POLITEHNICA from Bucharest, e-mail: catalina.petrescu@upb.ro

² Faculty of Electrical Engineering, University POLITEHNICA from Bucharest, e-mail: lucian.petrescu@upb.ro

that the length l is much bigger then the other dimensions ($l \gg a$, $l \gg b$), considering for the calculus as infinite long conductors.

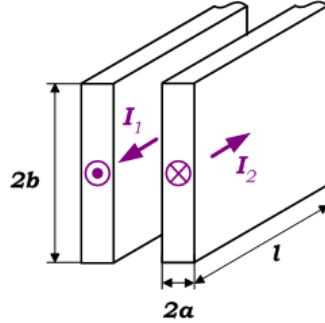


Fig. 1. DC Busbar distribution systems

2. Magnetic Field Analysis of a DC Rectangular Conductor

First, we will consider a rectangular bar with the cross section ($2a \times 2b$). The plan-parallel electromagnetic problem will generate a magnetic flux density vector in the plan xOy of the cross section considered. Applying the Biot-Savart-Laplace [8] formula, the \mathbf{B} components in a point $P(x,y)$ in the busbar proximity can be found [9] - Fig. 2:

$$\begin{aligned} d^2 B_x &= \frac{\mu_0 I}{8\pi ab} \frac{y - y_0}{(x - x_0)^2 + (y - y_0)^2} dx_0 dy_0 \\ d^2 B_y &= \frac{\mu_0 I}{8\pi ab} \frac{x - x_0}{(x - x_0)^2 + (y - y_0)^2} dx_0 dy_0 \end{aligned} \quad (1)$$

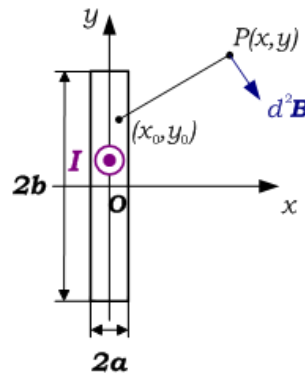


Fig. 2. Cross section of a rectangular bar

Using equation (1), the module of the vector potential at any point nearby the rectangular bar is [9]:

$$A = \frac{\mu_0 I}{8\pi ab} \int_{-a-b}^a \int_{-b}^b \frac{dx_0 dy_0}{\ln \sqrt{[(x - x_0)^2 + (y - y_0)^2]}} \quad (2)$$

Integrating and simplifying, (2) becomes:

$$\begin{aligned} A = & \frac{\mu_0 I}{8\pi ab} \{ (a-x)(b-y) \ln [(a-x)^2 + (b-y)^2] + \\ & + (a+x)(b-y) \ln [(a+x)^2 + (b-y)^2] + \\ & + (a+x)(b+y) \ln [(a+x)^2 + (b+y)^2] + \\ & + (a-x)(b+y) \ln [(a-x)^2 + (b+y)^2] + \\ & + (a-x)^2 \left(\operatorname{arctanh} \frac{b-y}{a-x} + \operatorname{arctanh} \frac{b+y}{a-x} \right) + \\ & + (a+x)^2 \left(\operatorname{arctanh} \frac{b-y}{a+x} + \operatorname{arctanh} \frac{b+y}{a+x} \right) + \\ & + (b-y)^2 \left(\operatorname{arctanh} \frac{a-x}{b-y} + \operatorname{arctanh} \frac{a+x}{b-y} \right) + \\ & + (b+y)^2 \left(\operatorname{arctanh} \frac{a-x}{b+y} + \operatorname{arctanh} \frac{a+x}{b+y} \right) \} \end{aligned} \quad (3)$$

The components of the magnetic flux density will be determined as follow:

$$\begin{cases} B_x = \frac{\partial A}{\partial y} \\ B_y = -\frac{\partial A}{\partial x} \end{cases} \quad (4)$$

Accordingly, the total value of the magnetic flux density is then:

$$B = \sqrt{B_x^2 + B_y^2} \quad (5)$$

For validating these expressions a comparison between the above analytical formulas integrated in common symbolic software (Maple) [10] and the numerical simulation by a free 2D software (FEMM) [11] was performed.

We choose a rectangular bar with the cross section of 360 mm^2 ($a = 3 \text{ mm}$ and $b = 30 \text{ mm}$). This kind of busbar supports in DC over 869 A and for the simulations we had use a rated current of 800 A. The simulations were made assuming $y = 0$ in both situations. The results are presented in Fig. 3.

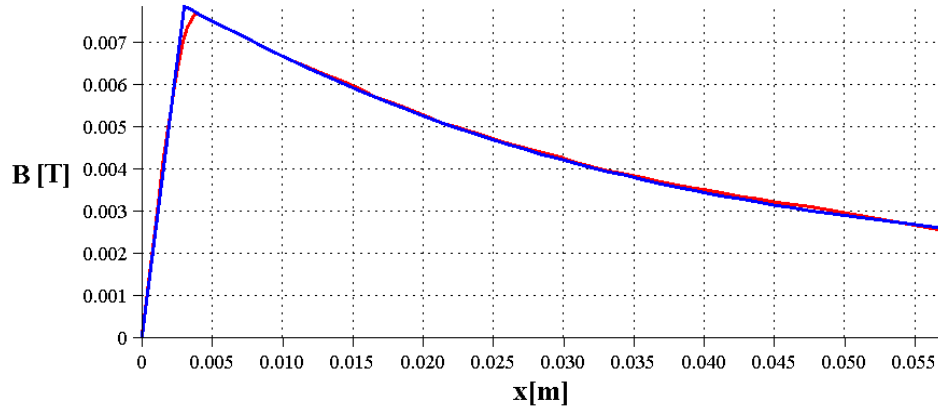


Fig. 3. Comparison between the magnetic flux density variation using the analytical approach (blue) and the numerical simulation (red)

The magnetic flux density spectrum for the rectangular conductor is shown in Fig. 4.

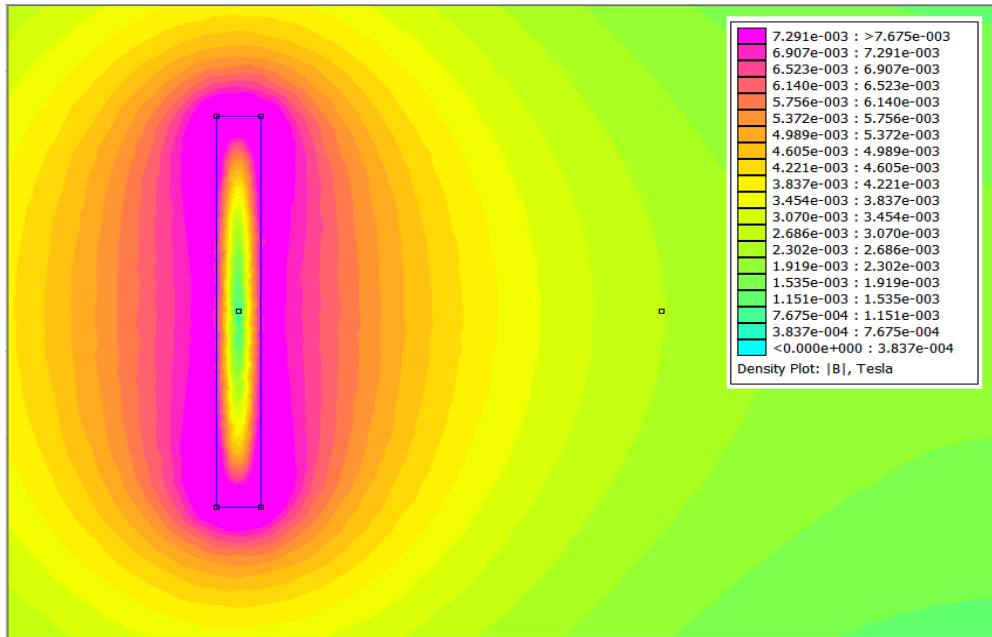


Fig. 4. Magnetic flux density spectrum for a rectangular conductor.

3. Magnetic Field of a System with Two DC Conductors

Using the superposition analysis of the static fields, the magnetic flux density between two rectangular conductors was evaluated. These two conductors are part of a busbar distribution system powered with DC currents.

Further we will consider also the distance d between the centers of the conductors on the horizontal direction –Fig. 5.

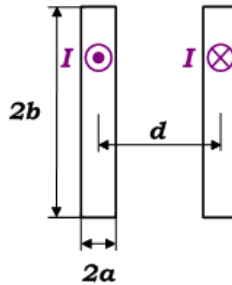


Fig. 5. Busbar distribution system composed of two rectangular conductors.

The study was carrying out for three different values of the distance between the centers of the conductors: $d (= 4a) = 12$ mm, $d (=8a) = 24$ mm and $d (=12a) = 36$ mm respectively.

In Fig. 6 one can observe the magnetic flux density spectrum between the bars

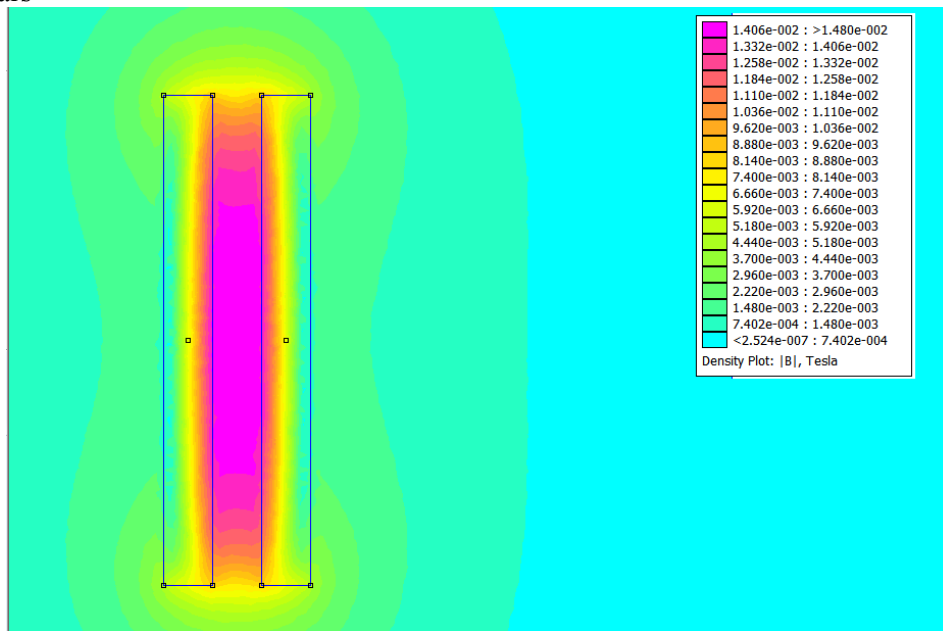


Fig. 6. Magnetic flux density spectrum for the distance of 12 mm between the bars

While Fig. 7 presents a comparison between the analytical and numerical computed values of the magnetic field density \mathbf{B} over the distance $d = 12$ mm between the centers of the conductors.

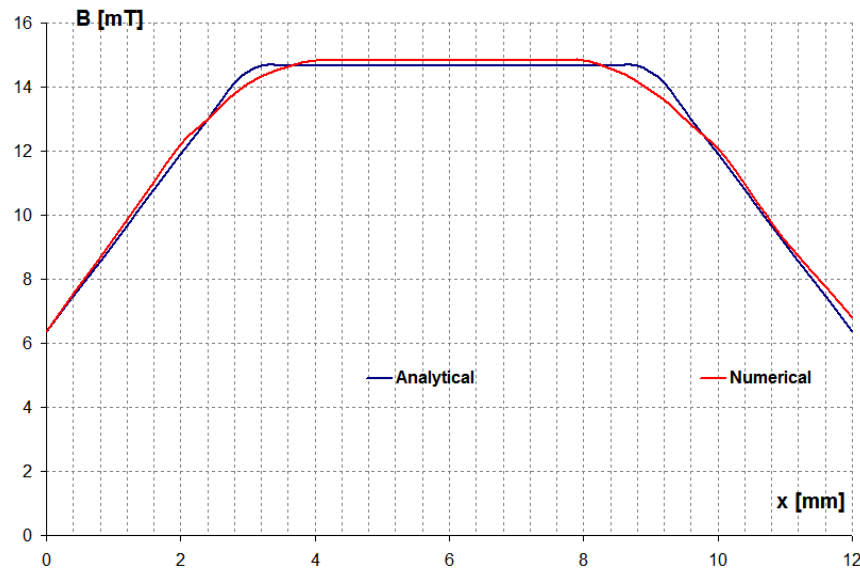
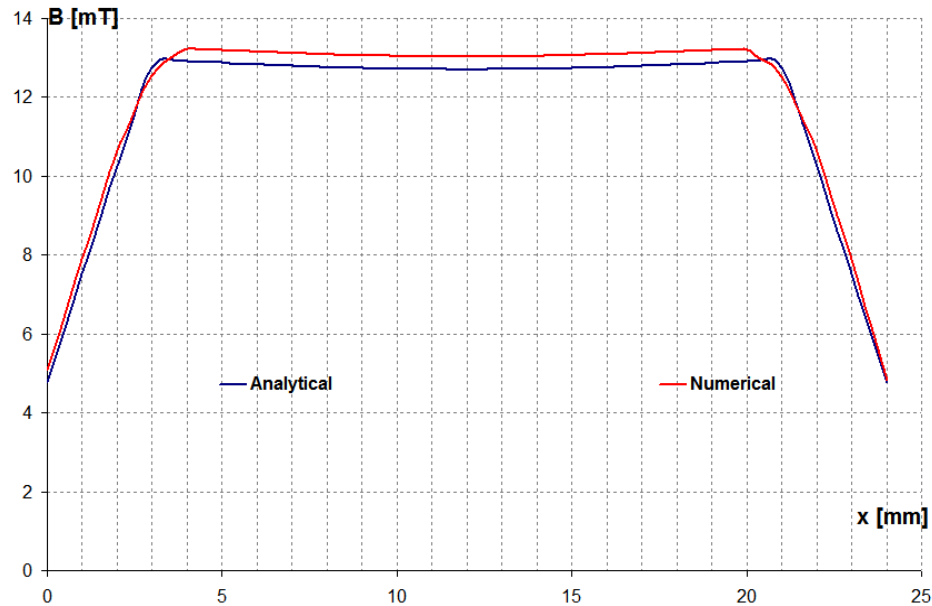
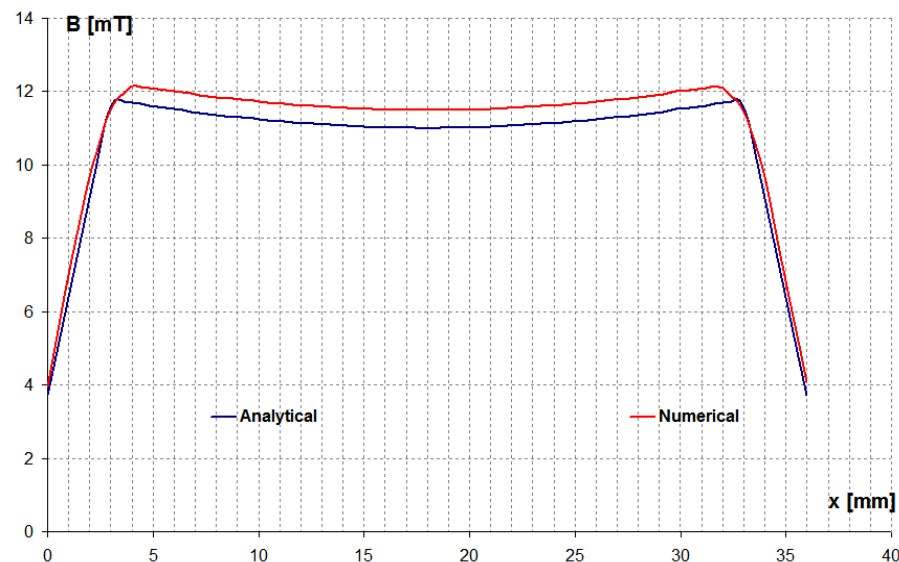


Fig. 7. Comparison between the magnetic flux density values, computed by numerical and analytical methods, over the distance $d = 12$ mm between the centers of the conductors

In Figs. 8 and 9 the comparative variations for the magnetic flux density between the bars for other two different distances: $d = 24$ mm and $d = 36$ mm are presented.

Fig. 8. Comparison between the computed magnetic flux density for $d = 24$ mmFig. 9. Comparison between the computed magnetic flux density for $d = 36$ mm

The relative error between the maximum values of the magnetic flux density, evaluated with (6), and the average relative errors for these values on the distance d , for each case studied computed with (7), were performed:

$$\varepsilon_r(B_{\max}) = \left| \frac{B_{\max_analytical} - B_{\max_numerical}}{B_{\max_analytical}} \right| \cdot 100 [\%] \quad (6)$$

and

$$\varepsilon_r(B) = \frac{1}{n} \sum_{k=1}^n \left| \frac{B_{analytical} - B_{numerical}}{B_{analytical}} \right| \cdot 100 [\%] \quad (7)$$

where, n is the number of the calculation and modeling points for the distance between the busbars.

These relative errors are presented in table 1.

Table 1
Relative errors between analytical and numerical value for the magnetic flux density

| Studied Case | Distance d [mm] | $\varepsilon_r(B_{\max})$ [%] | $\varepsilon_r(B)$ [%] |
|--------------|-------------------|-------------------------------|------------------------|
| 1 | 12 | 1.13 | 1.7 |
| 2 | 24 | 2.06 | 2.7 |
| 3 | 36 | 3.38 | 4.5 |

4. Electrodynamiс Forces Determination for the DC Busbar System

The final part of the study is focused on the analytical and numerical determination of the electrodynamical forces between these two bars of the DC distribution system. The analytical approach uses some simplifying assumptions: the height of the conductor is much bigger then its width ($2b \gg 2a$), the distance between the conductors is much bigger then their width ($d \gg 2a$).

Considering these, the force that acts on the second conductor, due to the current from the first one, is to be computed with the following relation [12]:

$$F_d = \frac{\mu_0}{2\pi} I_1 I_2 \frac{l}{d} \varphi(d, b), \quad (8)$$

where

$$\varphi(d, b) = \frac{d^2}{4b^2} \left[\frac{4b}{d} \operatorname{arctanh} \frac{2b}{d} - \ln \left(1 + \frac{4b^2}{d^2} \right) \right] \quad (9)$$

is also known as the Dwight formula.

The numerical determination of the force was made using one conductor in FEMM and selecting the Lorentz Force option (Fig. 10).

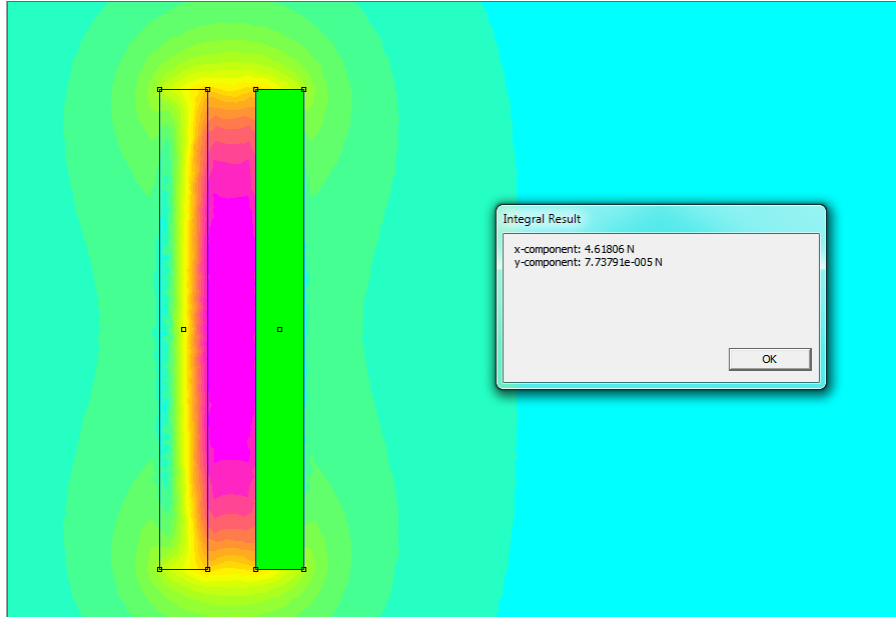


Fig. 10. Numerical determination of the electrodynamic force in FEMM for the distance of 12 mm between the bars

In both analytical and numerical determinations, we considered the unit length l of the bars (per unit meter). As it was expected, the vertical component of the force is much less than the horizontal one. In table 2, the forces calculated with formula (8), their numerical values determined with FEMM and their relative errors using (6) are presented.

Table 2
Relative errors between analytical and numerical value for the electrodynamic forces

| Studied Case | Analytical value F_{an} [N] | Numerical value F_{num} [N] | $\varepsilon_r (F)$ [%] |
|--------------|-------------------------------|-------------------------------|-------------------------|
| 1 | 4.469 | 4.618 | 3.21% |
| 2 | 3.388 | 3.656 | 7.34% |
| 3 | 2.695 | 3.086 | 12.69% |

It can be observed that a higher distance between the conductors generates a higher value of the relative error between the two determined forces.

In Fig. 11 is presented a variation of the force between the conductors as a function of the two parameters indicated in equation (9): height of the conductors and the distance between them.

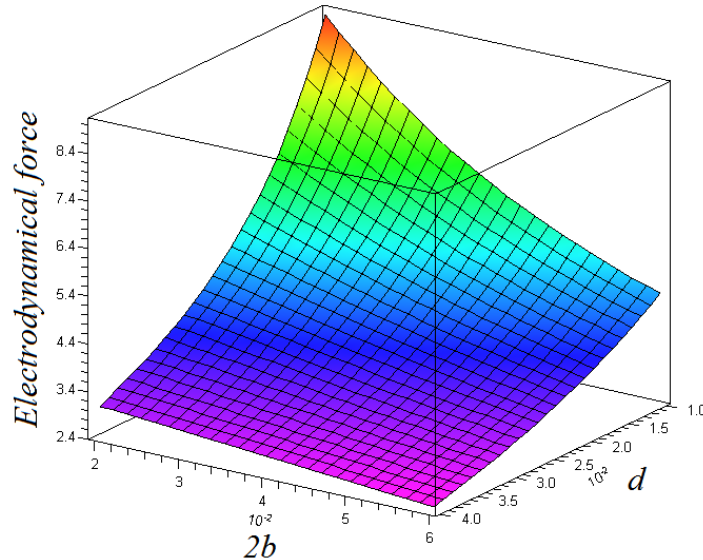


Fig. 11. Variation of the electrodynamic forces between the conductors as function of height and the distance between them

These forces are more important to be determined in transient fault regime of the busbar rather than the rated one. As it can be observed in Table 2, the values of these forces are very weak even for rated current of 800 A. On the other hand, in a short-circuit regime, these forces increase with the square of the current value, so this may lead to damages for the busbar system.

In table 3 are presented the values of the forces analytically determined for the rated current of 800 A and for a presumed short-circuit current of 8 kA.

Table 3
Electrodynamical forces in a busbar system working with rated currents, respectively in a short-circuit situation

| Studied Case | Rated value for $I=800\text{A}$ F_n [N] | Short-circuit value for $I=8\text{kA}$ F_{sc} [N] |
|--------------|---|---|
| 1 | 4.469 | 446.972 |
| 2 | 3.388 | 338.811 |
| 3 | 2.695 | 269.498 |

5. Conclusions

The paper studied the magnetic flux density spectrum, which was determined by analytical equations and by numerical techniques for a single

rectangular conductor and for a DC busbar system made by two rectangular conductors. The results were very alike as it was graphically shown (Fig. 3, 7, 8 and 9) for different situations and also using relative errors (Table 1).

The main objective of the paper was to determine the electrodynamic forces between the conductors in a rated regime of high DC currents, using an analytical formula and numerical computations. The results presented in Table 2 indicate that, for a small distance between the conductors, the relative error is very feeble. For a distance of 10 times the conductor's width, the error between the forces numerically and analytically computed increases over 10%.

The study has its relevance for a transient regime like a short-circuit when the current increases over 10 times.

R E F E R E N C E S

- [1]. *Gaoyu Zou, Zhengming Zhao, Liqiang Yuan*, Study on DC busbar structure considering stray inductance for the back-to-back IGBT-based converter, Applied Power Electronics Conference and Exposition (APEC), 2013 Twenty-Eighth Annual IEEE, 2013, p. 1213-1218.
- [2]. *Buschendorf, M.; Kobe, M.; Alvarez, R.; Bernet, S.*, Comprehensive design of DC busbars for medium voltage applications, IEEE Energy Conversion Congress and Exposition (ECCE), 2013, p. 1880-1885.
- [3] *E. Cazacu, Marilena Stănculescu* – On the stability issues of the main electromagnetic levitation techniques, The Sci. Bull. of the Elect. Eng. Fac., year 13, No. 1(21), pp. 9 – 13, 2013.
- [4]. <http://www.metalex.cl/>.
- [5]. *Popa, I.; Dolan, A.I.*, Numerical modeling of DC busbar contacts, 13th International Conference on Optimization of Electrical and Electronic Equipment (OPTIM 2012), p. 188 – 193, 2012.
- [6]. *Yongsug Suh; Changwoo Kim*, A Study on High-Current Rectifier Systems With Mitigated Time-Varying Magnetic Field Generation at AC Input and DC Output Busbars, IEEE Transactions on Power Electronics, vol. 27 (3), p. 1212-1219, 2012.
- [7]. *C. Lazaroiu , C. Bulac , M.O. Popescu , N. Golovanov*, Control and protection of a multiterminal low voltage dc system based on VSC, U.P.B. Sci. Bull., Series C, Vol. 74, Iss. 1, 2012, p. 173 – 180.
- [8]. *E. Cazacu, I. V. Nemoianu, M. C. Constantin* – Accurate Computation of the Prospective Short Circuit Currents in Low Voltage Electric Installations, EEA, Vol. 59, Nr. 1, 2011, pp. 41–48.
- [9]. *C. Mocanu*, Teoria Campului Electromagnetic, Editura Didactica și Pedagogică, București, 1984.

- [10]. <http://www.maplesoft.com/>.
- [11]. <http://www.femm.info/wiki/HomePage>.
- [12]. *G. Hortopan*, Aparate Electrice de Comutație – vol. I. Principii, Editura tehnică, București, 2000.